Submitted to Physics and Chemistry of Minerals 5/5/2002

First Principles Based Calculations of the $CaCO_3 - MgCO_3$ and $CdCO_3 - MgCO_3$ Subsolidus Phase Diagrams

B.P. Burton[1] and A. Van de Walle[2]

[1]*Materials Science and Engineering Laboratory, Ceramics Division National Institute of Standards and Technology, Gaithersburg, MD 20899, USA; benjamin.burton@nist.gov*

[2]*Materials Science and Engineering Department, Northwestern University 633 Clark Street Evanston, IL 60208, USA; avdw@northwestern.edu*

Abstract

Planewave pseudopotential calculations of supercell total energies were used as bases for first principles calculations of the $CaCO_3 - MgCO_3$ and $CdCO_3 - MgCO_3$ phase diagrams. Calculated phase diagrams are in qualitative to semiquantitative agreement with experiment, with the exception that two unobserved phases $Cd_3Mg(CO_3)_4$ and $CdMg_3(CO_3)_4$ are predicted. No new phases are predicted in the $CaCO_3 - MgCO_3$ system, but a low lying metastable $Ca_3Mg(CO_3)_4$ state, analogous to the $Cd_3Mg(CO_3)_4$ phase is predicted. All of the predicted lowest lying metastable states have dolomite related structures; i.e. they are layer structures in which A_mB_n cation layers lie perpendicular to the rhombohedral [111] vector.

Key words: First Principles, phase diagram calculation, order-disorder, $CaCO_3 - MgCO_3$, $CdCO_3 - MgCO_3$.

I. INTRODUCTION

Experiments by Goldsmith and coworkers (Goldsmith and Heard 1961, Goldsmith 1972, Goldsmith 1983) elucidated phase relations in the systems calcite-magnesite, $X \cdot CaCO_3 - (1-X) \cdot MgCO_3$, and otavite-magnesite, $X \cdot CdCO_3 - (1-X) \cdot MgCO_3$ (X = mol fraction $MgCO_3$) and established the characteristic phase diagram topology: A relatively narrow homogeneity range for an ordered dolomite structure phase that transforms by a second-order transition to a disordered calcite structure phase; Broad calcite + dolomite two-phase fields flank the dolomite homogeneity range. Previous phase diagram calculations (Navrotsky and Louks 1977, Burton and Kikuchi 1984, Burton 1987, Burton and Davidson 1988) for these, and related systems (e.g. $CaCO_3 - FeCO_3$, Davidson 1994) were based on empirically derived Hamiltonians (sets of energy parameters) and directed towards: 1) finding a minimal model that qualitatively reproduces phase diagram topology; 2) fitting experimental phase equilibria and thermochemical data (Navrotsky and Capobianco 1987, Capobianco et al. 1987, Chai et al. 1995). This paper presents first principles (FP) phase diagram (FPPD) calculations in which cluster expansion (CE) Hamiltonians (Sanchez et al. 1984, McCormack and Burton 1997) are fit to sets of supercell total energies ($\{E_{Str}\}$, where Str indicates the crystal structure) that were calculated with a plane wave pseudopotential code (Kresse and Hafner 1993).

The calcite crystal structure (calcite, otavite, magnesite) can be idealized as interpenetrating face centered cubic (fcc) substructures of cations (Ca^{2+}, Cd^{2+}, Mg^{2+}) and planar CO_3^{2-} anion groups. One $[111]_{fcc}$ vector becomes the rhombohedral 3-fold axis ($[111] \equiv [111]_{fcc} = [111]_{rhom} = [0001]_{hex}$) because the planes defined by CO_3-groups lie in the perpendicular (111) plane [$(111) \equiv (111)_{fcc} = (111)_{rhom} = (0001)_{hex}$]. In the dolomite structure [$CaMg(CO_3)_2$ and $CdMg(CO_3)_2$] alternating (111) planes are occupied by different cations (e.g. dolomite, Ca-Mg-Ca-...) which reduces space group symmetry from $R\bar{3}c$ in calcite to $R\bar{3}$ in dolomite. In both calcite and dolomite, the CO_3-groups are ordered such that groups on neighboring (111)-planes are oriented in an opposite sense.

In the $CaCO_3 - MgCO_3$ system, some additional ordered superstructures have been predicted as possible equilibrium phases (Burton 1987), or reported as metastable phases in natural samples of magnesian calcite, calcian dolomite, or ankerite [$Ca(Fe, Ca, Mg)(CO_3)_2$ with dolomite structure] (Van Tendeloo et al. 1985, Wenk and Zhang 1985, Meike et al 1988, Reksten 1990a, 1990b, 1990c) Several superstructures can be described in terms of analogous FCC-based ordered alloy structures [Burton and Davidson 1988, Wenk et. al. (1991); Table I]. Huntite ($\mathcal{H}'$; Graf and Bradley, 1962) has $CuAu_3$-type cation ordering as in μ', but it also has a distinct structure and space group symmetry because its CO_3-groups are ordered differently than those in calcite, dolomite or other superstructures considered here. There are also dolomite-related layer structures that consist of various sequences of Ca- and Mg-rich layers perpendicular to [111]; Table II.

Two factors that significantly affect carbonate phase relations are ignored in this study: (1) CO_3-group orientationl order-disorder; (2) quasiternary cation substitutions. The former is known to occur in $CaCO_3$ (and magnesian calcite) which exhibits a phase transition at $\sim 1260K$ (Dove and Powell, 1989). Such transitions have not been reported in $CdCO_3$ or $MgCO_3$. Factor (2) above primarily effects the comparison of FPPD calculations for the pure $CaCO_3 - MgCO_3$ systems with electron microscopy studies of natural samples that contain significant concentrations of transition metals, particularly Fe; e.g. the atural samples described in Wenk et al. (1991) have compositions $Ca_{0.5}Mg_{0.2}Fe_{0.3}CO_3$ and $Ca_{0.95}Mg_{0.05}CO_3$.

TABLE I: FCC-Related Crystal Structures.

Name[a]	Symbol[b]	X	*SpaceGroup*[c]	FCC-Related Prototype
α	$\bullet$	0	$R\bar{3}c$	FCC calcite
γ	∇	$\frac{1}{4}$	$P\bar{1}$	Cu_3Pt
ζ	$\blacktriangle$	$\frac{1}{4}$	$C2/c$	Al_3Ti
μ	$\times$	$\frac{1}{4}$	$R\bar{3}c$	Cu_3Au
ν	$\circ$	$\frac{1}{2}$	$C2/c$	$CuAu$
β	$\blacksquare$	$\frac{1}{2}$	$R\bar{3}$	$CuPt$ dolomite
$\mathcal{H}'$	$\triangleleft$	$\frac{3}{4}$	$R32$	$CuAu_3$ *Huntite*[d]

[a] A complimentary structure in which Ca or Cd is replaced by Mg and vice versa, is distinguished by a primed name; e.g μ is $Ca_3Mg(CO_3)_4$ $(X = \frac{1}{4})$, μ' is $CaMg_3(CO_3)_4$ $(X = \frac{3}{4})$.

[b] Symbols used in Figures 1 and 2.

[c] Space group determinations were performed with the Cerius program.

[d] Huntite has $CuAu_3$-type cation order as in μ', but its CO_3-groups are differently ordered than those in calcite, dolomite or other supercells considered here.

TABLE II: Dolomite-Related Layer Structures.

Name	Symbol	X	Space Group	[111]-Layer Sequence	Notation[a]
η	+	$\frac{1}{6}$	$P\overline{3}$	$M^1 - C^1 - C^2 - C^3 - C^4 - C^5 - M^1 - ...$	$[111]_{C_5M}$
ϵ	□	$\frac{1}{4}$	$R\overline{3}$	$M^1 - C^1 - C^2 - C^3 - M^1 - ...$	$[111]_{C_3M}$
δ	♦	$\frac{1}{3}$	$P\overline{3}$	$C^1 - M^1 - C^2 - C^3 - C^4 - M^1 - C^1 - ...$	$[111]_{CMC_3M}$
β	■	$\frac{1}{2}$	$R\overline{3}$	$C^1 - M^1 - C^1 - ...$ dolomite	$[111]_{CM}$

[a] C = Ca- or Cd-layer, M = Mg-layer.

The prediction in Burton (1987) was for a possible low-temperature equilibrium $Ca_3Mg(CO_3)_4$ phase with either μ (Cu_3Au) or ζ (Al_3Ti) related ordering, or a combination of the two (Burton and Davidson, 1988). Wenk et. al. (1991) report the unequivocal observation of δ in calcian dolomite, and suggest that γ is most probably the source of "**c**-reflections," which occur halfway between fundamental reflections along a_1 hexagonal (e.g. at $h - \frac{1}{2}hl$, Table 2 in Van Tendaloo et al. 1982) and are associated with intralayer ordering, in magnesian calcite; ν-type ordering is also proposed as a possible cause of "**c**-reflections." The FP and FPPD results presented below include formation energies for all these structures, and assuming that cation ordering is the only relevant process: 1) Predict no stable intermediate phases between calcite and magnesite; 2) Confirm that δ is a low energy candidate for metastable formation from calcian dolomite; 3) Appear to rule out γ, μ, ν, and ζ as plausible candidates for metastable formation; 4) Predict that ϵ is the lowest lying metastable state at $X = \frac{1}{4}$.

II. TOTAL ENERGY CALCULATIONS

Total energies, E_{Str}, were calculated for $CaCO_3$, $CdCO_3$, $MgCO_3$, and many $Ca_mMg_n(CO_3)_{(m+n)}$ and $Cd_mMg_n(CO_3)_{(m+n)}$ supercells. All calculations were performed with the Vienna *ab initio* simulation program (VASP; Kresse et al 1993) using ultrasoft Vanderbilt type plane-wave pseudopotentials (Vanderbilt 1990) with a local density approximation for exchange and correlation energies. Electronic degrees of freedom were optimized with a conjugate gradient algorithm, and both cell constant and ionic positions were fully relaxed. Valence electron configurations for the pseudopotentials are: $Ca\ 6p^26s^2$; $Cd5s^24d^{10}$; $Mg\ 2p^63s^2$; $C\ 2s^22p^2$; $O\ 2s^22p^4$. Total energy calculations were converged with respect to k-point meshes; 112 symmetrically distinct k-points was typical for 30 or 40-atom triclinic supercells. An energy cutoff of 400 eV was used, in the "high precision" option which guarantees that *absolute* energies are converged to within a few meV (a few tenths of kJ/mol; mol = a mole of exchangeable cations; Ca^{2+}, Cd^{2+}, Mg^{2+}).

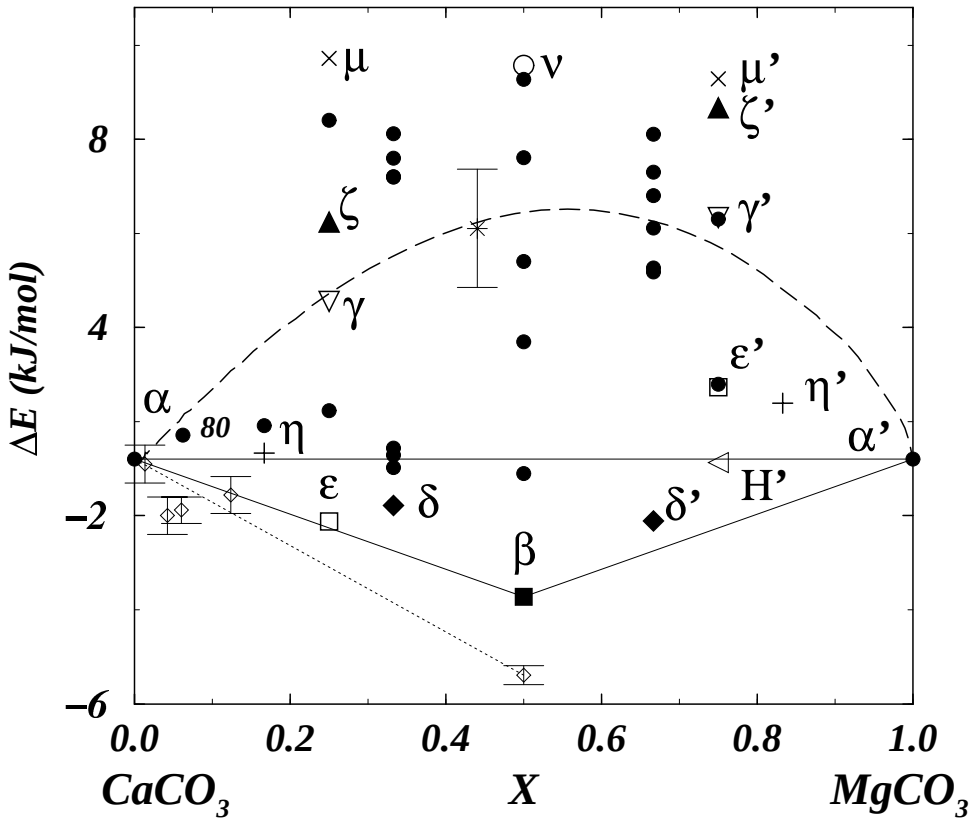

FIG. 1: $CaCO_3 - MgCO_3$: Comparison of VASP calculated formation energies ΔE_{Str}, (Str indexes a crystal structure and X = mol fraction $MgCO_3$) with experimental heats of formation. $\diamond$ with error bars = Navrotsky and Capobianco (1987) data; Dotted line connects calcite with the lowest-energy measurement for dolomite. * with error bars is data of Chai et al. (1995) for their most disordered dolomite sample. The dashed line is the FPPD calculated total energy for a random solid solution, $\Delta E_{Rand}(X)$. The solid line connects predicted ground state structures: α=calcite; β=dolomite; α'=magnesite.

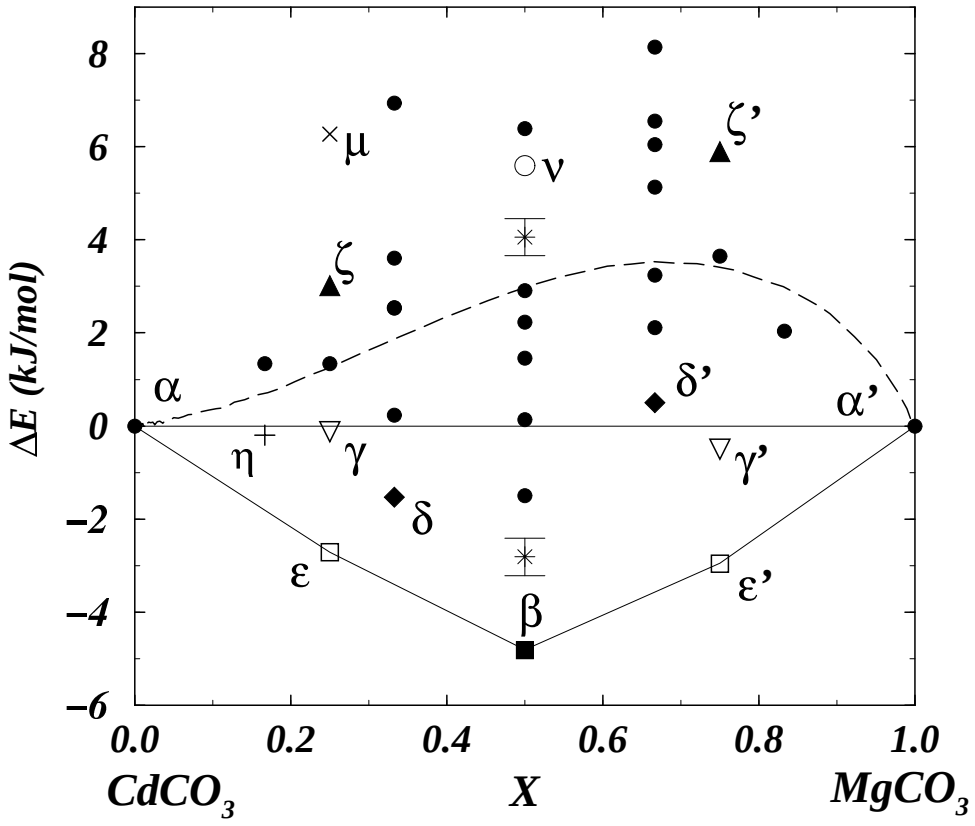

FIG. 2: $CdCO_3 - MgCO_3$. Comparison of VASP calculated formation energies ΔE_{Str}, experimental heats of formation. * with error bars = data of Capobianco et al. (1987) for maximally ordered, and disordered β-phase. The dashed line is the FPPD calculated total energy for a random solid solution, $\Delta E_{Rand}(X)$. The solid line indicates predicted ground state structures: α=calcite; ϵ=$[111]_{C_3M}$; β=dolomite; ϵ'=$[111]_{CM_3}$; α'=magnesite.

Results of the FP total energy calculations are listed as formation energies, ΔE_{Str}, in Table III which also describes supercell cation configurations. Formation energies are defined such that ΔE_{Str} for a $Ca_m Mg_n (CO_3)_{(m+n)}$ supercell with crystal structure Str is:

$$\Delta E_{Str} = \frac{E_{Str} - mE_{\alpha} - nE_{\alpha'}}{m+n} \tag{II.1}$$

where E_{Str} has units of energy/supercell, but ΔE_{Str}, E_{α} and $E_{\alpha'}$ have units of energy/cation. The ΔE_{Str} are compared with calorimetric data (Navrotsky and Capobianco, 1987; Capobianco et al. 1987; Chai et al. 1995) in Figures 1 and 2. Experimental heats of formation for magnesian calcite with $0 \leq X < 0.05$, are lower than a mechanical mixture of calcite plus dolomite (dotted line) which implies a tendency for ordering in this composition range. Explicitly investigating this range with FP calculations requires supercells with at least 100, atoms and such calculations have not been attempted; one high symmetry Ca-rich 80-atom supercell calculation was performed, but it has a positive formation energy, $\Delta E_{80} = 0.64\ kJ/mol$.

TABLE III: Calculated formation energies for $Ca_mMg_n(CO_3)_{(m+n)}$ and $Cd_mMg_n(CO_3)_{(m+n)}$ supercells; all energies are in kJ/mol.

M:N Name Order-type	T-Matrix[a]	Cation Coordinates	Ion Mg=0	Ca_mMg_n ΔE_{Str} $\Delta E_{Str'}$[b]	Cd_mMg_n ΔE_{Str} $\Delta E_{Str'}$
2 : 0	1 0 0	0 0 0	1	0^Y	0^Y
Calcite	0 1 0	1/2 1/2 1/2	1	0^Y	0^Y
$\alpha - fcc$	0 0 1				
15 : 1	2 0 0	0 0 0	0	0.64	
	0 2 0	1/2 0 0	1		
	0 0 2	0 1/2 0	1		
		0 0 1/2	1		
		0 1/2 1/2	1		
		1/2 0 1/2	1		
		1/2 1/2 0	1		
		1/2 1/2 1/2	1		
		1/4 1/4 1/4	1		
		1/4 1/4 3/4	1		
		1/4 3/4 1/4	1		
		3/4 1/4 1/4	1		
		1/4 3/4 3/4	1		
		3/4 1/4 3/4	1		
		3/4 3/4 1/4	1		
		3/4 3/4 3/4	1		
5 : 1	1 0 0	1/2 3/2 -3/2	1	0.90	1.34

	1 -1 -1	1/2 1/2 -1/2	1		
	-1 2 -1	0 1 -1	1		
		1/2 1/2 -3/2	1		
		1 1 -2	1		
		1 0 -1	0		
5 : 1	-1 1 0	-1 0 -1	1	0.16	-0.20
η	0 1 -1	-1/2 1/2 -1/2	1		
$[111]_{5:1}$	-1 -1 -1	-3/2 1/2 -3/2	1		
		-3/2 3/2 -3/2	1		
		-1 1 -1	1		
		-2 1 -2	0		
3 : 1	0 1 -1	-3/2 1/2 1/2	1	1.30^Y	1.33^Y
	0 -1 0	-1 0 0	1	6.38^Y	3.65^Y
	-2 1 1	-1/2 1/2 -1/2	1		
		-2 1 0	0		
3 : 1	1 -1 0	1/2 1/2 1/2	1	-1.65^Y	-2.71^Y
ϵ	0 1 -1	1 0 0	1	1.92^Y	-2.96^Y
$[111]_{3:1}$	0 1 1	1/2 1/2 -1/2	1		
		1 1 0	0		
3 : 1	0 -1 1	1/2 -1/2 3/2	1	4.19^Y	-0.12^Y
γ	1 0 0	0 0 1	1	6.42^Y	-0.50^Y
Cu_3Pt	-1 1 1	-1/2 1/2 3/2	1		
		0 0 2	0		
3 : 1	3/2 -1/2 -1/2	0 0 0	0	44.73	
$\mathcal{H}$	-1/2 3/2 -1/2	0 1 -1	1	-0.09	
Huntite[c]	-1/2 -1/2 3/2	-1 0 1	1		
Cu_3Au		1 -1 0	1		

6 : 2	1 1 -1	-1 0 -1	1	10.65	6.27
μ	-1 1 1	-1/2 1/2 -1/2	1	10.11	
Cu_3Au	1 -1 1	-3/2 1/2 -3/2	1		
		-3/2 3/2 -3/2	1		
		-1 1 -1	1		
		-1 1 -1	1		
		-1 1 -1	0		
		-2 1 -2	0		
6 : 2	1 1 -1	-1 0 -1	1	4.60	3.02
ζ	-1 1 1	-1/2 1/2 -1/2	1	9.34	5.90
Al_3Ti	1 -1 1	-3/2 1/2 -3/2	1		
		-3/2 3/2 -3/2	1		
		-1 1 -1	1		
		-1 1 -1	1		
		-1 1 -1	0		
		-2 1 -2	0		
6 : 2	1 1 -1	-1 0 -1	1	17.03	
ζ^h	-1 1 1	-1/2 1/2 -1/2	1		
Al_3Ti^c	1 -1 1	-3/2 1/2 -3/2	1		
		-3/2 3/2 -3/2	1		
		-1 1 -1	1		
		-1 1 -1	1		
		-1 1 -1	0		
		-2 1 -2	0		
4 : 2	-1 1 0	0 2 -1	1	7.50^Y	6.94^Y
43	0 0 1	-1/2 3/2 -1/2	1	7.63^Y	5.14^Y
48	1 2 -2	0 1 0	1		

		1/2 3/2 -1/2	1		
		1/2 5/2 -3/2	0		
		0 3 -1	0		
4 : 2	0 1 -1	2 0 -1	1	0.29^{Y}	-1.59^{Y}
13	0 1 0	3/2 3/2 -3/2	1	5.08^{Y}	3.24^{Y}
18	3 -1 -1	3 1 -2	1		
		1/2 1/2 -1/2	1		
		5/2 1/2 -3/2	0		
		1 1 -1	0		
4 : 2	-1 0 1	-1/2 -3/2 1/2	1	8.65^{Y}	3.61^{Y}
24	-1 1 -1	-1 0 0	1	8.64^{Y}	8.14^{Y}
28	1 -2 0	-1 -1 0	1		
		-1/2 -1/2 1/2	1		
		0 -1 0	0		
		-1/2 -1/2 -1/2	0		
4 : 2	1 0 0	1/2 1/2 -1/2	1	0.11^{Y}	0.24^{Y}
32	1 -1 -1	1/2 1/2 -3/2	1	4.98^{Y}	2.12^{Y}
37	-1 2 -1	1 1 -2	1		
		1/2 3/2 -3/2	1		
		1 0 -1	0		
		0 1 -1	0		
4 : 2	1 0 0	0 1 -1	1	7.51^{Y}	2.54^{Y}
31	1 -1 -1	1/2 1/2 -3/2	1	6.15	6.05
38	-1 2 -1	1 1 -2	1		
		1/2 3/2 -3/2	1		
		1/2 1/2 -1/2	0		
		1 0 -1	0		

4 : 2	1 0 0	1 0 -1	1	8.00^{Y}	2.53^{Y}
33	1 -1 -1	1/2 1/2 -3/2	1	7.01^{Y}	6.55^{Y}
35	-1 2 -1	1 1 -2	1		
		1/2 3/2 -3/2	1		
		1/2 1/2 -1/2	0		
		0 1 -1	0		
4 : 2	-1 1 0	-1 0 -1	1	-1.23	-1.53
δ	0 1 -1	-3/2 3/2 -3/2	1	-1.64	0.50
$[111]_{CMC_3M}$	-1 -1 -1	-1 1 -1	1		
		-2 1 -2	1		
		-1/2 1/2 -1/2	0		
		-3/2 1/2 -3/2	0		
1 : 1	1 0 0	0 0 0	1	-3.66^{Y}	-4.82^{Y}
Dolomite	0 1 0	1/2 1/2 1/2	0		
$\beta - CuPt$	0 0 1				
2 : 2	0 1 -1	-1/2 1/2 -1/2	1	8.27^{Y}	2.91^{Y}
1	0 -1 0	-1 0 0	1		
	-2 1 1	-3/2 1/2 1/2	0		
		-2 1 0	0		
2 : 2	1 -1 0	1/2 1/2 1/2	1	-0.38^{Y}	-1.50^{Y}
4	0 1 -1	1 0 0	1		
	0 1 1	1/2 1/2 -1/2	0		
		1 1 0	0		
2 : 2	0 -1 1	-1/2 1/2 3/2	1	8.02^{Y}	5.60^{Y}
ν	1 0 0	0 0 1	1		
$CuAu$	-1 1 1	1/2 -1/2 3/2	0		

		0 0 2	0		
2 : 2	0 -1 1	-1/2 1/2 3/2	1	8.02^Y	1.45^Y
8	1 0 0	0 0 2	1		
	-1 1 1	1/2 -1/2 3/2	0		
		0 0 1	0		
3 : 3	0 1 -1	1 1 -1	1	10.09^Y	6.39^Y
15	0 1 0	3 1 -2	1		
	3 -1 -1	1/2 1/2 -1/2	1		
		2 0 -1	0		
		5/2 1/2 -3/2	0		
		3/2 3/2 -3/2	0		
3 : 3	-1 0 1	-1/2 -1/2 -1/2	1	5.25^Y	0.14^Y
23	-1 1 -1	-1 -1 0	1		
	1 -2 0	-1/2 -1/2 1/2	1		
		0 -1 0	0		
		-1/2 -3/2 1/2	0		
		-1 0 0	0		
3 : 3	-1 1 0	0 1 0	1	3.13^Y	2.23^Y
45	0 0 1	0 3 -1	1		
	1 2 -2	1/2 3/2 -1/2	1		
		0 2 -1	0		
		1/2 5/2 -3/2	0		
		-1/2 3/2 -1/2	0		

[a]Matrix T defines supercell lattice constants, relative to rhombohedral calcite [$R\bar{3}c$ cell constants: *a and* α; $Ca:\ (0,0,0)$; $C:\ (1/4,1/4,1/4)$; $O:\ (x,1/2-x,1/4),\ x=0.507$] (Megaw, 1973). such that the inverse of the transpose of T, $t \equiv [T^t]^{-1}$, transforms listed cation coordinates (column 3) into fractional supercell coordinates, e.g. for δ-phase:

$$T = \begin{vmatrix} -1 & 1 & 0 \\ 0 & 1 & -1 \\ -1 & -1 & -1 \end{vmatrix} \Rightarrow [T^t]^{-1} \bullet \begin{vmatrix} -1 \\ 0 \\ -1 \end{vmatrix} = \begin{vmatrix} -2/3 & 1/3 & 1/3 \\ 1/3 & 1/3 & -2/3 \\ -1/3 & -1/3 & -1/3 \end{vmatrix} \bullet \begin{vmatrix} -1 \\ 0 \\ -1 \end{vmatrix} = \begin{vmatrix} 1/3 \\ 1/3 \\ 2/3 \end{vmatrix}$$

[b] ΔE_{Str} is the formation energy for a $Ca_m Mg_n (CO_3)_{(m+n)}$ supercell, and $\Delta E_{Str'}$ is for the complimentary $Ca_n Mg_m (CO_3)_{(m+n)}$ supercell: $\Delta E_\epsilon = -1.65\ kJ/mol$ for $Ca_3 Mg (CO_3)_4$; $\Delta E_{\epsilon'} = 1.92\ kJ/mol$ for $CaMg_3 (CO_3)_4$.

[c] Huntite, $\mathcal{H}' = CaMg_3 (CO_3)_4$, and ζ^h have differently ordered CO_3-groups than calcite, dolomite or other superstructures listed in this table.

[Y] The Y (Yes) superscript is attached to each ΔE_{Str} and $\Delta E_{Str'}$ that was used to fit the effective cluster interactions (ECI).

III. FIRST PRINCIPLES PHASE DIAGRAM CALCULATIONS

A Fitting the Cluster Expansion

The cluster expansion (CE) Sanchez et al. (1984) is a compact representation of the alloys' configurational total energy. In the quasi-binary systems studied here, the alloy configuration is described by pseudospin occupation variables σ_i, which take values -1 or $+1$ depending upon which cation occupies site i; $\sigma_i = -1$ for Ca or Cd, $\sigma_i = +1$ for Mg.

The CE parametrizes the configurational energy (per atom) as a polynomial in pseudospin occupation variables:

$$E(\sigma) = \sum_{\ell} m_\ell J_\ell \left\langle \prod_{i \in \ell'} \sigma_i \right\rangle \tag{III.1}$$

where ℓ is the cluster defined by the set of sites $\{i\}$. The sum is taken over all clusters ℓ that are not symmetrically equivalent in the parent lattice space group, and the average is taken over all clusters ℓ' that are symmetrically equivalent to ℓ. Coefficients J_ℓ are called effective cluster interactions (ECI), and the *multiplicity* of a cluster, m_ℓ, is the number of symmetrically equivalent clusters, divided by the number of lattice sites. The ECI are obtained by fitting a set of FP calculated structure energies, $\{E_{Str}\}$. The resulting CE can be improved as necessary by increasing the number of clusters ℓ and/or the number of E_{Str} used in the fit.

Fitting was performed with the MIT Ab-initio Phase Stability software package (MAPS; van de Walle 1999) which automates most of the tasks associated with the construction of a CE Hamiltonian. A complete description of the algorithms underlying the code can be found in (van de Walle and Ceder 2002). The most important steps are: 1) Selecting which FP structure energies to calculate, which MAPS does in a way that minimizes the statistical variance of the estimated ECI; 2) Automatically selecting which clusters to include in the expansion by minimizing the *cross-validation score*, CV:

$$(CV)^2 = \frac{1}{N}\sum_{Str=1}^{N}(E_{Str} - \hat{E}_{-Str})^2 \qquad \text{(III.2)}$$

where $E_1, \ldots E_N$ denote the structure energies calculated from FP and E_{-Str} is the energy of structure *Str predicted from a CE* fitted to the remaining $N-1$ energies. This criterion ensures that the chosen set of clusters maximizes the predictive power of the CE for any structure, whether or not it is included in the fit. (In contrast, the standard mean square error criterion only minimizes the error for structures included in the fit.) In addition to the CV-criterion, the code also ensures that ground states predicted from the CE agree with the minimum energy structures for each composition, as calculated from FP. The code proceeds by iterative refinement, gradually increasing the number of clusters and the number of structures to provide the best possible fit based on the set $\{E_{Str}\}$ calculated so far.

For this study, MAPS was run until CE-precision reached CV=0.015 meV/cation for the $CaCO_3 - MgCO_3$ system and CV=0.019 meV/cation for $CdCO_3 - MgCO_3$. Achieving this accuracy required calculation of the 27 E_{Str} that are marked by the superscript Y in Table III.

The end result of this procedure is a set of ECI, $\{J_{(r,t)}\}$, which define the interactions associated with r-body clusters of types t. Fitted ECI sets for $CaCO_3 - MgCO_3$ and $CdCO_3 - MgCO_3$ are listed in Table IV, and the products of effective pair interactions [EPI; $J_{(2,t)}$] and their multiplicities, $m_{(r,t)}$, are plotted in Figure 3: $\bullet$ = values for $CaCO_3 - MgCO_3$; $\square$ = values for $CdCO_3 - MgCO_3$. As postulated by Burton and Kikuchi (1984), $J_{(2,1)}$, the nearest neighbor (nn) *interlayer* pair interaction favors ordering while $J_{(2,2)}$, the nn *intralayer* interaction favors phase separation; note that the sign convention is reversed relative to Burton and Kikuchi (1984); here $J_{(2,1)} > 0$ favors ordering and $J_{(2,2)} < 0$ favors phase separation.

TABLE IV: Effective Cluster Interactions in kJ/mol.

Rhombohedral Cluster Coordinates minus (0,0,0)	m(r,t) Multiplicity	$CaCO_3 - MgCO_3$	$CdCO_3 - MgCO_3$
Zero Cluster	1	13.150425	5.957591
Point Cluster	2^I	1.862754	2.741019
(1/2,-1/2,1/2)	6	0.450299	1.208615
(0,-1,1)	6	-1.828504	-1.649628
(1/2,-3/2,1/2)	6	0.313948	0.674401
(1,0,0)	6	-0.283364	0.056055
(-3/2,3/2,-1/2)	12	-0.619792	-0.574350
(1,1,-1)	6	0.016498	
(1,-2,1)	6	-0.452398	
(-1/2,0,-1/2), (-1/2,-1/2,1/2)	12	-0.390458	-0.26610
(-1,0,1), (0,-1,1)	4	0.624520	-0.38727

^{I} 2 is the multiplicity of cations in the Z=2 rhombohedral cell.

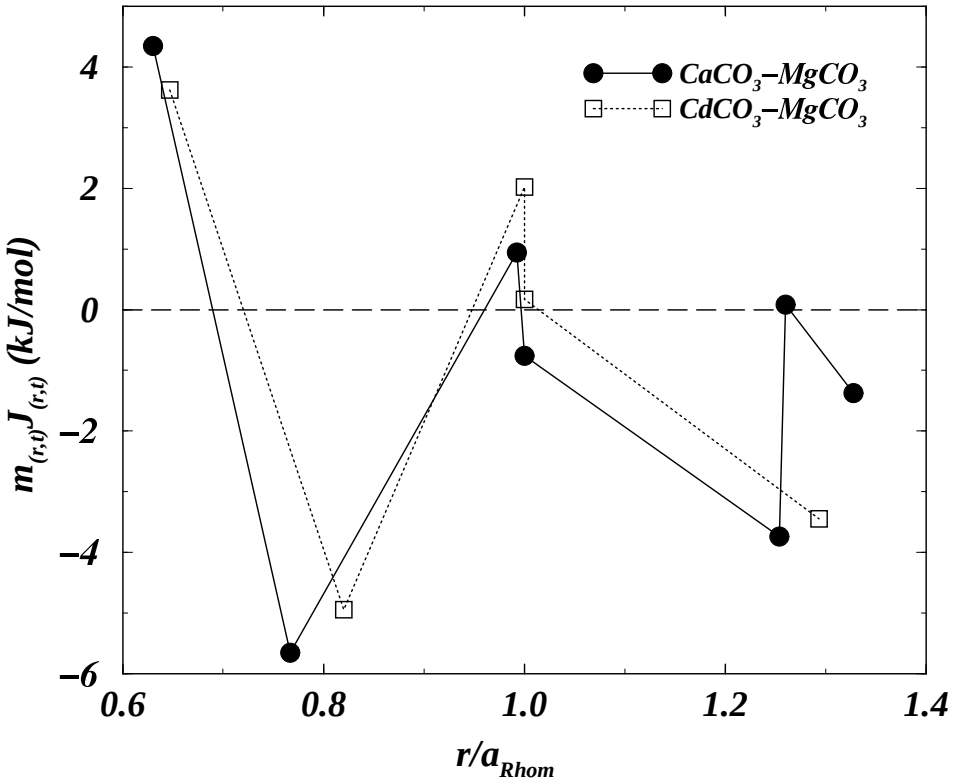

FIG. 3: Effective pair interactions, $J_{(2,t)}$, multiplied by their multiplicities, $m_{(r,t)}$, for • $CaCO_3-MgCO_3$ and □ $CdCO_3-MgCO_3$. The sign convention is: $J_{(2,1)} > 0$ implies that *interlayer* ordering is energetically favorable; $J_{(2,2)} < 0$ implies that *intralayer* ordering is energetically unfavorable (as postulated by Burton and Kikuchi, 1984).

B Ground State Analysis

Ground-state (GS) analyses were performed by brute force enumeration of all ordered configurations with 60 or fewer atoms per supercell (12 or fewer cation sites). These analyses did not predict any new GS configurations besides those shown in Figures 1 and 2. In addition, Monte Carlo (MC) simulations described below revealed no other ground states, strongly suggesting that our ground state search is exhaustive.

C Monte Carlo Phase Diagram Calculations

The MAPS package includes a companion MC code (described in van de Walle and Asta, 2002) that was used to calculate the $CaCO_3 - MgCO_3$ and $CdCO_3 - MgCO_3$ phase diagrams (Figures 4 and 5). This code implements semi-grand canonical Monte Carlo simulations, in which the total number of atoms is fixed and the chemical concentration varies in response to to a fixed difference in the chemical potentials of the two cation species. Phase boundaries at a given temperature were found by scanning a range of imposed chemical potential values while monitoring the concentration in the simulation cell. Phase transitions were located by identifying discontinuities in the concentration. Values of the concentration just before and just after the discontinuity bracketed the equilibrium concentrations of coexisting phases at the transition.

Convergence with respect to system size was tested by calculating T_c for the $\beta \rightleftharpoons \alpha$, dolomite$\rightleftharpoons$calcite, order-disorder transition, and a system of 12x12x12 supercells (3465 cation sites) was selected for all MC calculations. Thermodynamic functions of interest, such as concentration, were obtained by averaging over 1500 MC passes for each value of chemical potential and temperatures. Temperature and chemical potential were scanned in increments of 5 K and 0.01 eV/atom, respectively. After each detected phase transition, the system was re-equilibrated for 1500 MC passes before the process of locating the phase boundary at the next temperature was initiated.

IV. DISCUSSION

A Equilibrium Phase Relations: Comparison with experiment

Qualitatively, there are no discrepancies between predicted and experimental phase diagrams. The unobserved ϵ, and ϵ' phases in $CdCO_3 - MgCO_3$ are predicted to occur only at temperatures below the lowest that were investigated experimentally. Predicted values for the critical temperatures of $\beta \rightleftharpoons \alpha$ order-disorder transitions at $X = 0.5$ are:

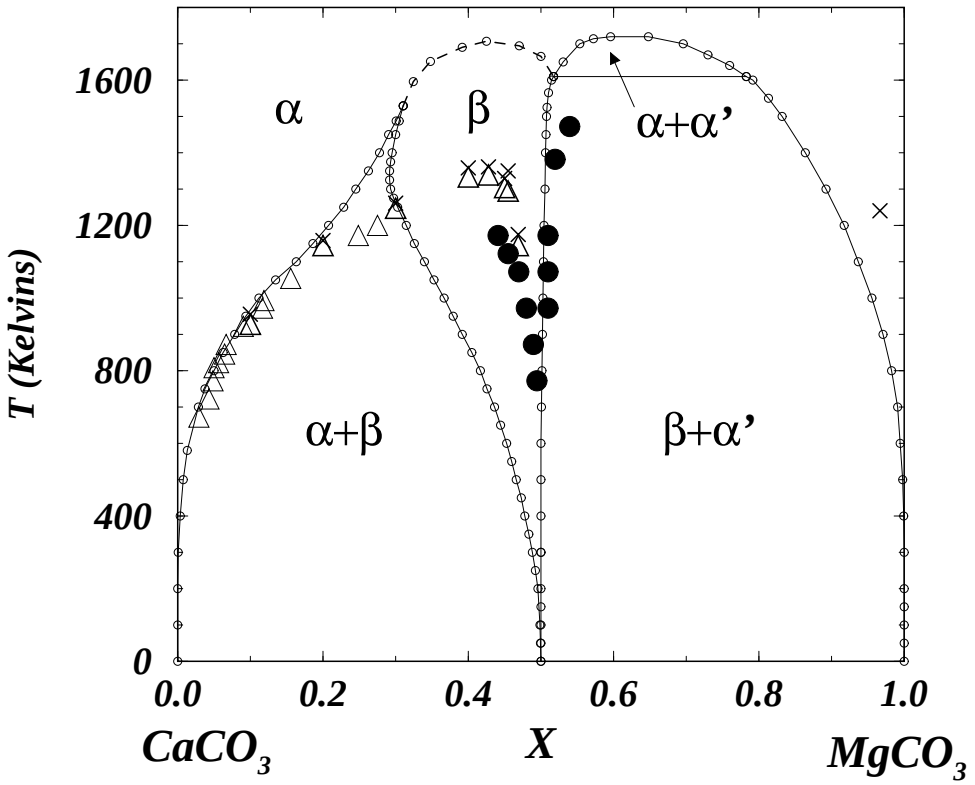

FIG. 4: Calculated $CaCO_3 - MgCO_3$ phase diagram (solid and dashed lines through small open circles). Experimental phase boundary data are from Goldsmith, 1983 and references therein.

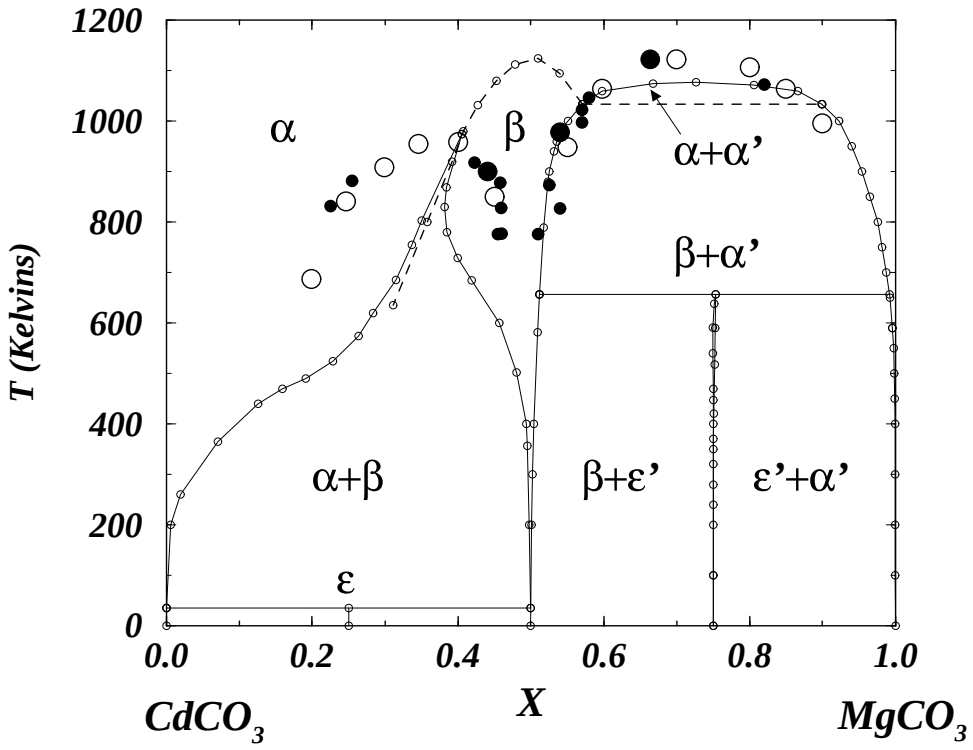

FIG. 5: First principles based calculation of the $CdCO_3 - MgCO_3$ phase diagram (solid and dashed lines through small open circles). Large open circles and filled circles are data from Goldsmith and Heard 1972.

$T_C(Predicted)/T_C \approx 1.16 \pm 0.03$ for $CaCO_3 - MgCO_3$, and $T_C(Predicted)/T_C \approx 1.04 \pm 0.02$ for $CdCO_3 - MgCO_3$. Typically, FPPD calculations overestimate transition temperatures especially when, as here, vibrational effects are ignored; e.g. $T_C(Predicted)/T_C \approx 1.32$ for the compound CdMg, Asta et al. (1993).

Solubilities of Ca, or Cd, in the dolomite structure β-phases are significantly overestimated. In addition, the predicted $CaCO_3 - MgCO_3$ homogeneity range for α' is enhanced, and the field for two Mg-rich disordered phases is reduced, relative to the experimental diagram.

B Metastable Phase Relations: Magnesian Calcite and Calcian Dolomite

Assuming that cation ordering is the only relevant process, the ΔE_{Str} results plus the $\Delta E_{Rand}(X)$ curve (dashed line, Figure 4) provide a substantially improved basis for interpreting metastable phase relations in magnesian calcite and calcian dolomite (Wenk et al 1991). Metastable ordered phases have a driving force for formation only if their free energies are lower than that of the disordered solution from which they might form; i.e. $F_{Ord} < F_{Rand}$ is a *necessary*, but not sufficient, condition for metastable formation. Because the random state has greater configurational entropy than any ordered configuration (or any disordered phase with short range order) and it will therefore have lower free energy than any ordered state of equal or higher formation energy, at finite temperature. It follows that:

$$\Delta E_{Ord} > \Delta E_{Rand} \Rightarrow F_{Ord} > F_{Rand} \qquad \text{(IV.1)}$$

which implies that $\Delta E_{Ord} < \Delta E_{Rand}$ is a *necessary* condition for an ordered phase to be a candidate for metastable formation. Thus, all phases with $\Delta E_{Str} > \Delta E_{Rand}(X)$ (μ, ν, ζ), or $\Delta E_{Str} \approx \Delta E_{Rand}(X)$, ($\gamma$) are poor candidates for metastable formation. These results clearly contradict all proposed models of ordering in magnesian calcite with $X \approx \frac{1}{4}$: 1) the

proposal of Wenk et al (1991) that "**c**-reflections" in magnesian calcite might be caused by ν-type ordering; 2) predictions of Burton (1987) and Burton and Davidson (1988) that a μ- or ζ-type ordering, or a combination of the two, might actually be associated with a stable low-temperature phase. The lowest energy metastable states are all dolomite related layer structures: δ, $[111]_{CMC_3M}$; ϵ, $[111]_{C_3M}$; η, $[111]_{C_5M}$ Table I. From an energetic perspective, it is surprising that ϵ-type ordering has not been reported in magnesian calcite; ϵ is predicted to be very nearly stable, and it is substantially more stable than any of the previously predicted candidates.

Predictions of Burton (1987) "that $Ca_3Mg(CO_3)_4$ is probably stable at low temperature," meaning a phase with μ- or ζ-type cation order, or a combination of the two, (Burton and Davidson, 1988) are apparently wrong. This prediction was based on a cluster variation method (CVM; Kikuchi 1951) calculation in the tetrahedron approximation (TA), that could only include the first two EPI [$J_{(2,1)}$ and $J_{(2,2)}$], nn *interlayer* and *intralayer* pair interactions, plus one three-body term. The Hamiltonian fit by MAPS, however, includes the first seven EPI plus two three-body terms. Clearly the CVM TA is not sufficient for this system because the largest included clusters are too small, and this demonstrates the advantage of using MC simulation for FPPD calculations; MC calculations easily handle relatively long-range interactions, whereas CVM expansions typically become intractable when interaction range exceeds third- or fourth-nn.

Wenk et al (1991) used a concentration wave (CW) analysis (Khachaturyan 1978, Khachaturyan and Pokrowskii 1985, Khachaturyan et al. 1988) as a basis for discussing metastable phase relations between α, β, γ, δ, μ, and ν, phases (ignoring ϵ and ζ). The CW criterion for a plausible transition between two phases (e.g. $\beta \rightarrow \gamma$) is that the two structures be sufficiently similar that they *may* be related by a "simple instability;" i.e. an infinitesimal perturbation in the amplitude of *one* ordering CW which reduces the free energy of the system. This criterion combines two concepts: 1) structural similarity; 2) instability with respect to a change in ordering. The latter criterion implies a negative second derivative of the free energy with respect to order parameters, i.e. ordering waves. The

CW analysis however, provides no Hamiltonian with which to evaluate formation energies, free energies, or instabilities, and these are severe limitations. Also, the $\alpha \rightarrow \epsilon$ reaction is associated with a "simple instability," $\mathbf{k}_\epsilon = \frac{2\pi}{a}[\frac{1}{3}(111)_{fcc}]$ in the notation of Wenk et al (1991), and because its energy is so low, one would expect it to proceed readily. However, ϵ is only associated with unobserved **d**-reflections ($hkl : -h+k+l \neq 3n$, Table 2 in Van Tendeloo et al. 1985) rather than the observed **c**-reflections.

The FPPD results establish an energy hierarchy which rules out most proposed metastable ordering processes: e.g. $\Delta E_\gamma \approx \Delta E_{Rand}$, and $\Delta E_\beta \gg \Delta E_\delta$ so $\beta \rightarrow \gamma$ in calcian dolomite is a highly unlikely reaction, but $\beta \rightarrow \delta$ is highly plausible. Some caveats related to CO_3-group disorder and impure samples: (1) CO_3-group disorder would increase the energy of disordered magnesian calcite, or metastable calcian dolomite, and this could make some high-energy states accessible as metastable reaction products. CO_3-group disorder in magnesian calcite is plausible because the 1260K order-disorder transition temperature (Dove and Powell 1989) implies energetics that are comparable to cation order-disorder, however, disordered natural samples with higher energy than ΔE_{Rand} have not been reported. (2) Natural samples that exhibit sharp **c**-reflections with streaking (Wenk et al. 1991) are very Fe-rich, $Ca_{0.5}Mg_{0.2}Fe_{0.3}CO_3$, which may have a significant effect on thier energetics. Samples of composition $Ca_{0.95}Mg_{0.05}CO_3$ also exhibit **c**-reflections, but they are more diffuse and streaking is not observed.

C Predicted Phases in $CdCO_3 - MgCO_3$

In the $CdCO_3 - MgCO_3$ system, both the ϵ- and ϵ'-phases are predicted to be stable, but neither has been observed experimentally. This does not contradict experiment however, because the highest temperature at which ϵ' is predicted to be stable is $\sim 650K$ which is $\sim 40K$ below the lowest temperature experiments reported in Goldsmith and Heard (1972).

V. CONCLUSIONS

The results presented above demonstrate semiquantitative agreement between FPPD calculations and experimental phase equilibria and thermochemical data. They also provide an energetic hierarchy that can be used to evaluate the plausibilities of proposed metastable reaction paths. Specifically, the FP and FPPD results presented above appear to rule out the proposed metastable formation of γ or ν in magnesian calcite, unless the magnesian calcite is disordered with respect to *both* cation ordering and CO_3-group orientation. Low-temperature ϵ- and ϵ'-phases are predicted in the $CdCO_3 - MgCO_3$ system.

VI. ACKNOWLEDGEMENTS

This work was partially supported by NSF contract DMR-0080766, and NIST.

VII. REFERENCES

Asta, M., McCormack, R. and de Fontaine, D. (1993) Theoretical study of alloy phase stability in the Cd-Mg system. Physical Review **B48**: 748-766.

Burton, B.P. and Kikuchi, R. (1984) Thermodynamic analysis of the system $CaCO_3 - MgCO_3$ in the tetrahedron approximation of the cluster variation method. American Mineralogist **69**: 165-175.

Burton, B.P. (1987) Theoretical analysis of cation ordering in binary rhombohedral carbonate systems, American Mineralogist, **72**: 329-336 (see also note added in proof).

Burton, B.P. and Davidson, P.M. (1988) Multicritical phase relations in minerals; in **Advances in Physical Geochemistry** vol. 7, pp 60-90, edited by S. Ghose, J.M.D. Coey and E. Salje. Springer-Verlag New York.

Capobianco, C., Burton, B.P., Davidson, P.M., and Navrotsky, A. (1987) Structural and calorimetric studies of order-disorder in $CdMg(CO_3)_2$. Journal of Solid State Chemistry **79**: 214-223.

Chai, L., Navrotsky, A. and Reeder, R.J. (1995) Energetics of calcium-rich dolomite, Geochemica et Cosmochemica Acta, **59**[5]: 939-944.

Davidson, P.M. (1994) Ternary iron, magnesium, calcium carbonates: A thermodynamic model for dolomite as an ordered derivative of calcite-structure solutions, American Mineralogist **79**: 332-339.

Dove, M.T. and Powell, B.M. (1989) Neutron diffraction study of the tricritical orientational order/disorder phase transition in calcite at 1260K, Phys. Chem Minerals **16**: 503-507.

Goldsmith, J.R. and Heard, H.C. (1961) Subsolidus phase relations in the system $CaCO_3 - MgCO_3$, Journal of Geology, **69**: 453-457.

Goldsmith, J.R. (1972) Cadmium dolomite and the system $CdCO_3 - MgCO_3$. J. Geol. **80**: 611-626.

Goldsmith, J.R. (1983) Phase relations of rhombohedral carbonates; in **Reviews in Mineralogy**: vol. 11. edited by R.J. Reeder, pp 49-76. Mineralogical Society of America, Washington D.C.

Graf, D.L. and Bradley, W.F. (1962) The crystal structure of Huntite, $Mg_3Ca(CO_3)_4$. Acta Cryst. **15**: 238-242.

Khachaturyan, A.G. (1978) Ordering in substitutional and interstitial solid solutions. Prog. in Mater. Sci. **22**: 1-150.

Khachaturyan, A.G. and Pokrowskii, B.I. (1985) Concentration wave approach in structural and thermodynamic characterization of ceramic crystals. Prog. in Mater. Sci. **29**: 1-138.

Khachaturyan, A.G. Lindsley, T.F. and Morris, J.W. (1988) Theoretical investigation of precipitation of δ' in Al-Li. Metall. Trans. **19A**: 249-258.

Kikuchi, R. A theory of cooperative phenomena. Phys. Rev. **81**: 988-1003.

Kresse, G. and Hafner, J., Ab initio molecular dynamics for liquid metals Phys. Rev. **B47**: 558-561 (1993); Kresse, G. Thesis, Technische Universität Wien 1993; Phys. Rev. **B49**: 14 251 (1994). Kresse, G. and Furthmüller, J. (1996) Efficiency of ab-initio total energy calculations for metals and semiconductors using a plane-wave basis set Comput. Mat. Sci. **6**: 15-50; Efficient iterative schemes for ab initio total-energy calculations using a plane-wave basis set Phys. Rev. **B54**: 11169 (1996); cf. http://tph.tuwien.ac.at/ vasp/guide/vasp.html.

McCormack, R.P., Burton, B.P. Modeling phase stability in $A(B_{1/3}B'_{2/3})O_3$ perovskites, *Comp. Mater. Sci.* **8**: 153-160 (1997).

Megaw, HD, (1973) **Crystal Structures: A Working Approach**, Studies in Physics and Chemistry, **10**: W.B. Saunders Company, Philadelphia, London, Toronto, pp 242.

Meike, A. Wenk, H-R, O'Keefe, M.A. and Gronsky, R. (1988) Atomic resolution microscopy

of carbonates. Interpretation of contrast. Physics and Chemistry of Minerals **15**: 427-437.

Navrotsky, A. and Capobianco, C. (1987) Enthalpies of formation of dolomite and magnesian calcite. American Mineralogist **79**: 782-787.

Navrotsky, A. and Louks, D. (1977) Calculation of subsolidus phase relations in carbonates and pyroxenes, Physics Chemistry of Minerals **1**: 109-127.

Reksten, K. (1990a) Modulated microstructures in calcian ankerites. American Mineralogist **75**: 495-500.

Reksten, K. (1990b) Superstructures in calcite. American Mineralogist **75**: 807-812.

Reksten, K. (1990c) Superstructures in calcian ankerites. Physics and Chemistry of Minerals **17**: 266-270.

Sanchez, J.M., Ducastelle, F. and Gratias, D. (1984) Generalized cluster description of multicomponent systems Physica **128A**: 334-350.

van de Walle A. and G. Ceder (2002), Automating First-Principles Phase Diagram Calculations, Journal of Phase Equilibria, in press.

van de Walle A. and M. Asta (2002), Self-driven lattice-model Monte Carlo simulations of alloy thermodynamic, Submitted to Modelling and Simulations in Materials Science and Engineering.

van de Walle, A. (1999) MAPS: The MIT Ab initio Phase Stability code http://www.mit.edu/$\sim$ avdw/maps/

Vanderbilt, D. (1990) Soft self-consistent pseudopotentials in a generalized eigenvalue formalism Phys. Rev. **B41**: 7892-7895.

Van Tendeloo, G., Wenk, H.R. and Gronsky, R. (1985) Modulated structures in calcian dolomite: A study of electron microscopy. Physics and Chemistry of Minerals **12**: 333-341.

Wenk, H-R. and Zhang, F. (1985) Coherent transformations in calcian dolomites, Geology, **13**: 457-460.

Wenk, H-R. Meisheng, Hu, Lindsley, T, and Morris J.W. Jr. (1991) Superstructures in ankerite and calcite. Physics and Chemistry of Minerals **17**: 527-539.